Investigation of the Acoustic Boundary Layer in Porous-Walled Ducts with Flow

U. G. Hegde,* F. Chen,† and B. T. Zinn‡
Georgia Institute of Technology, Atlanta, Georgia

This paper investigates the acoustic boundary layer in porous-walled ducts with sidewall gas injection, a subject of interest in studies of a propellant driving in unstable solid-propellant rocket motors and sound attenuation in ducts. The formulation, valid for low injection Mach numbers, is two-dimensional and includes the effects of viscosity, thermal conductivity, and steady-state velocities. Solutions are provided for the first-order axial and transverse velocities and temperature in the boundary layer in terms of the acoustic pressure. It is shown that with an increase in the steady wall injection velocity, the acoustic boundary-layer thickness at a given frequency increases and its tendency to damp acoustic motions within the duct also increases. Experimental studies in a cylindrical, porous-walled duct confirm these trends and are reported. The analysis also shows that the acoustic admittance at the boundary-layer edge depends upon the axial location and varies most rapidly in regions adjacent to an acoustic pressure minimum.

Nomenclature

a	= defined by Eq. (31)
b	= norm of $L(y_0;y)$
c	= reference speed of sound
C_p	= specific heat at constant pressure
F,F_1	= defined by Eqs. (22), (24), and (25)
G	= Green's function for u_1' and T_1'
k	= thermal conductivity
K	= first modified version of the Green's function G
L	= second modified version of the Green's function G
L_m	= defined by Eq. (25)
m_1,m_2	= factors in the Green's function G
M	= core flow Mach number
p	= pressure
q	= modified v'
$R_b(0)$	= admittance at wall
$R_b(\infty)$	= admittance at edge of boundary layer
t	= time
T	= temperature
T_0',T_1'	= zeroth- and first-order temperature fluctuations
u	= velocity in axial direction
u_0',u_1'	= zeroth- and first-order axial velocity fluctuations
v	= velocity in transverse direction
V	= nondimensionalized injection velocity
x	= axial coordinate
$y,y_0,\tilde{y}$	= transverse coordinate
β	= defined by Eq. (15)
β_2	= parameter in Eq. (7)
γ	= ratio of specific heats
μ	= coefficient of viscosity
ν	= kinematic viscosity
λ	= parameter in integral equation for v'
ρ	= density
ω	= circular frequency

Superscripts

$(\ )^*$	= dimensional quantity
$(\ )'$	= fluctuation
$(\bar{\ })$	= steady state

Subscript

r	= reference value

Introduction

THE acoustic boundary layer in porous-walled ducts with flow is of interest in connection with admittance studies and instability analyses of solid-propellant rocket motors.[1,2] A porous-walled duct is similar to a solid rocket motor in that the mass addition from the sidewalls simulates the addition of gaseous products of combustion into the flow stream. The characteristics of the acoustic boundary layer are instrumental in determining the behavior of the acoustic waves in the duct. While the analysis presented in this paper is biased toward propulsion applications, it is also valid for studying the sound damping characteristics of acoustically nonrigid surfaces used in industry to damp unwanted noise from machinery and motor exhausts.[3] A porous wall, due to the dissipative effects in its pores, damps sound energy. However, the acoustic boundary layer present over such surfaces also contributes to the damping of the acoustic wave motion and must be also considered.

It is well known that acoustic wave motions in ducts with large length-to-diameter ratio are largely isentropic except in the vicinity of the duct walls, where the shear and thermal modes interact with the acoustic mode.[4] In the absence of mean flow, the thickness of the acoustic boundary layer is of the order of $(\nu^*/\omega^*)^{1/2}$, which is very small in many cases of practical interest. The acoustic admittance at the edge of the boundary layer, taking into account the effects of the shear and thermal modes, serves as a boundary condition for the isentropic wave motion away from the walls. Furthermore, when the boundary-layer thickness is much smaller than the transverse dimensions of the duct, the admittance may be applied directly at the side-walls without any significant loss in accuracy.

As discussed later in this paper, sidewall mass injection modifies both the thickness and structure of the acoustic boundary layer. The boundary-layer thickness is increased compared to the no-flow case and, if the injection rate is sufficiently high, the boundary layer may encompass a signifi-

Presented as Paper 85-0078 at the AIAA 23rd Aerospace Sciences Meeting, Reno, NV, Jan. 14-17, 1985; received April 11, 1985; revision received Jan. 6, 1986.

*Research Engineer, School of Aerospace Engineering.
†Visiting Scientist, School of Aerospace Engineering (from Northwestern Polytechnical University, Xian, China).
‡Regents' Professor, School of Aerospace Engineering. Associate Fellow AIAA.

cant portion of the duct. In such a case, the isentropic assumption for the core flow may lose validity and the viscous effects must then be included in the analysis of the whole flow region. However, for many cases of practical interest, the injection rate is sufficiently small so that boundary-layer assumptions should work well. These cases are investigated in this paper.

Different solution approaches are possible for this problem. Following Ref. 4, the velocity field may be split a priori into acoustic (potential) and vortical (solenoidal) modes that are then solved for separately. These solutions are combined only at the duct walls, where the no-slip boundary condition is applied to the overall velocity. The approach favored here does not, however, consider the acoustic, shear, and thermal modes separately. Instead, the boundary-layer equations are solved for the combined unsteady field. In the absence of turbulence effects in the main flow, the vortical modes disappear at the edge of the boundary layer, leaving only the potential velocities.

Flandro[1] carried out an analysis of the boundary layer in cold-flow rocket motors in an effort to provide corrections to experimentally obtained propellant admittances. T'ien[5] and, later, Flandro[6] included chemical reaction effects and numerically solved the boundary-layer equations. The admittances obtained by these investigations are independent of axial location within the combustor. The reason for this may be traced to the neglect of the axial mean flow velocities in the boundary-layer analysis. It is shown here that mean flow effects lead to an axial dependence of the acoustic admittance, particularly in regions of pressure minima. Nayfeh[7] investigated the acoustic boundary layer in rigid-walled ducts in the presence of an axial flow. He did not, however, consider flow injection into the duct as considered here. As mentioned earlier and as will be demonstrated, the injection velocity is of great importance in determining the acoustic boundary-layer thickness and structure.

Analysis

The region under consideration is a thin layer adjacent to the porous walls of a duct (Fig. 1). Constant-temperature gas is injected through the porous walls. Consequently, the steady flow has both transverse and axial steady-state velocities. The steady-state pressure, density, and temperature can be assumed to be constant at a given axial location and their variation with axial distance can be taken to be small, since only low Mach number flows will be considered. The Prandtl number is taken to be unity merely for convenience. A two-dimensional analysis is carried out using the boundary-layer equations. These are, in nondimensional form,[8]

$$\frac{\partial \rho}{\partial t}+\frac{\partial}{\partial x}\rho u+\frac{\partial}{\partial y}\rho v=0 \tag{1}$$

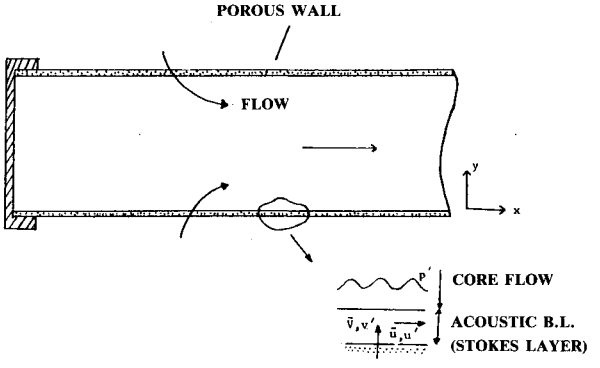

Fig. 1 Schematic of a porous-walled duct with sidewall mass addition.

$$\rho\left[\frac{\partial u}{\partial t}+u\frac{\partial u}{\partial x}+v\frac{\partial u}{\partial y}\right]=-\frac{1}{\gamma}\frac{\partial p}{\partial x}+\frac{\partial^2 u}{\partial y^2} \tag{2}$$

$$\frac{\partial T}{\partial t}+u\frac{\partial T}{\partial x}+v\frac{\partial T}{\partial y}=\frac{\gamma-1}{\gamma}\frac{\partial p}{\partial t}+\frac{\partial^2 T}{\partial y^2}+u\frac{\partial p}{\partial x} \tag{3}$$

$$p=\rho T \tag{4}$$

$$\frac{\partial p}{\partial y}=0 \tag{5}$$

In the above,

$$x=x^*\omega^*/c^* \qquad y=y^*\sqrt{\omega^*/\nu^*} \qquad t=t^*\omega^*$$

$$u=u^*/c^* \qquad v=v^*/\sqrt{\omega^*\nu^*}$$

$$T=T^*/T_r^* \qquad p=p^*/p_r^* \qquad \rho=\rho^*/\rho_r^*$$

$$\mu=\mu^*/\mu_r^*=1$$

Note that the transverse momentum equation has been replaced by Eq. (5). This implies that the core flow pressure is impressed upon the boundary layer. For the unsteady component of the pressure, this will be true if the acoustic waves are nearly planar, as will be assumed herein.

The dependent variables are now split into steady and unsteady components and a harmonic time dependence is assumed for the unsteady components. For example,

$$u=\bar{u}+u'e^{it}$$

It is also assumed that both

$$|u'|\ll 1$$

and

$$|\bar{u}|\ll 1$$

The steady-state version of Eq. (1) yields

$$\frac{\partial \bar{u}}{\partial x}+\frac{\partial \bar{V}}{\partial y}=0$$

The variation of $\bar{u}$, for low injection rates, occurs over a scale of the length of the duct. Correspondingly, the variation in $\bar{V}$ occurs over a length scale comparable to the cross-sectional dimension of the duct. Under the boundary-layer assumption, the thickness of the boundary layer is small compared to the cross-sectional dimension of the duct. Thus, in the boundary layer, it is sufficient to take

$$\bar{V}=\text{const} \tag{6}$$

Using this approximation and the steady-state continuity equation, it follows that $\partial\bar{u}/\partial x$ can be also neglected in the analysis. A reasonable approximation of $\bar{u}$ is given by[6]

$$\bar{u}=\bar{u}_c(1-e^{-\beta_2 y}) \tag{7}$$

where β_2 is a measure of the inverse of the axial, steady-velocity boundary-layer thickness.

The equations for the unsteady components are obtained by subtracting the steady-state equations from the conservation equations (1-5). Axial gradients of steady-state quantities (of the order of M^2) are neglected. Linearizing with respect to the unsteady flow variables the following equa-

tions are obtained:

$$\frac{\partial v'}{\partial y}-\bar{V}\frac{\partial T'}{\partial y}+\frac{\partial u'}{\partial x}+i(p'-T')+\bar{u}\frac{\mathrm{d}}{\mathrm{d}x}(p'-T')=0 \quad (8)$$

$$\frac{\partial^2 u'}{\partial y^2}-\bar{V}\frac{\partial u'}{\partial y}-iu'=\frac{1}{\gamma}\frac{\mathrm{d}p'}{\mathrm{d}x}+\frac{\partial \bar{u}}{\partial y}(v'+\bar{V}p'-\bar{V}T')+\bar{u}\frac{\partial u'}{\partial x} \quad (9)$$

$$\frac{\partial^2 T'}{\partial y^2}-\bar{V}\frac{\partial T'}{\partial y}-iT'=-i\left(\frac{\gamma-1}{\gamma}\right)p'-\left(\frac{\gamma-1}{\gamma}\right)\bar{u}\frac{\partial p'}{\partial x}+\bar{u}\frac{\partial T'}{\partial x} \quad (10)$$

$$\rho'=p'-T' \quad (11)$$

where use has been made of Eq. (11) in substituting for ρ' in Eqs. (8-10).

The boundary conditions at $y=0$ are taken as

$$v'(0)=R_b(0)p'$$

$$u'(0)=0 \text{ (no-slip condition)}$$

$$T'(0)=0 \text{ (assuming the wall to be isothermal)}$$

For convenience, the boundary conditions at the other end are specified at infinity. In practice, infinity is to be understood as the edge of the acoustic boundary layer whose thickness is yet to be determined. The boundary conditions may be derived to any order in M from the acoustic characteristics of the core flow, where the viscous effects and mean flow gradients may be neglected. For example, in the core flow, the acoustic momentum equation (9) becomes

$$iu'+\bar{u}\frac{\partial u'}{\partial x}=-\frac{1}{\gamma}\frac{\mathrm{d}p'}{\mathrm{d}x}$$

Expanding u' and T' in the following series:

$$u'=u_0'+u_1'+\ldots.$$

$$T'=T_0'+T_1'+\ldots.$$

where u_1' and T_1' are of order $(\bar{u}_c u_0')$ and $(\bar{u}_c T_0')$, respectively, it follows from the above momentum equation that u_0' and u_1' satisfy

$$iu_0'=-\frac{1}{\gamma}\frac{\mathrm{d}p'}{\mathrm{d}x}$$

and

$$iu_1'=-\bar{u}\frac{\partial u_0'}{\partial x}$$

Thus,

$$u_0'=\frac{i}{\gamma}\frac{\mathrm{d}p'}{\mathrm{d}x}$$

and to order (M)

$$u_1'=(\bar{u}/\gamma)p'$$

Hence, to order (M)

$$u'(\infty)=\frac{i}{\gamma}\frac{\mathrm{d}p'}{\mathrm{d}x}+\frac{\bar{u}_c p'}{\gamma}$$

and similarly

$$T'(\infty)=\left(\frac{\gamma-1}{\gamma}\right)p'$$

The solutions of Eqs. (8-10) will be obtained by a combination of perturbation and integral equation techniques. Toward this end, u' and T' in the boundary layer are again expanded in series similar to those given above. Substituting these into Eqs. (9) and (10), the following equations are obtained for u_0' and T_0' in the boundary layer:

$$\frac{\partial^2 u_0'}{\partial y^2}-\bar{V}\frac{\partial u_0'}{\partial y}-iu_0'=\frac{1}{\gamma}\frac{\mathrm{d}p'}{\mathrm{d}x} \quad (12)$$

$$\frac{\partial^2 T_0'}{\partial y^2}-\bar{V}\frac{\partial T_0'}{\partial y}-iT_0'=-i\left(\frac{\gamma-1}{\gamma}\right)p' \quad (13)$$

with the boundary conditions

$$u_0'(0)=T_0'(0)=0$$

$$u_0'(\infty)=\frac{i}{\gamma}\frac{\mathrm{d}p'}{\mathrm{d}x}$$

$$T_0'(\infty)=\left(\frac{\gamma-1}{\gamma}\right)p'$$

The solutions for u_0' and T_0' are obtained in a straightforward manner and are

$$u_0'=\frac{i}{\gamma}\frac{\mathrm{d}p'}{\mathrm{d}x}(1-\mathrm{e}^{-\beta y}) \quad (14)$$

and

$$T_0'=\left(\frac{\gamma-1}{\gamma}\right)p'(1-e^{-\beta y}) \quad (15)$$

where

$$\beta=(-\bar{V}+\sqrt{\bar{V}^2+4i})/2$$

The equations for u_1' and T_1' are

$$\frac{\partial^2 u_1'}{\partial y^2}-\bar{V}\frac{\partial u_1'}{\partial y}-iu_1'=\frac{\partial \bar{u}}{\partial y}(v'+\bar{V}p'-\bar{V}T_0')+\bar{u}\frac{\partial u_0'}{\partial x} \quad (16)$$

$$\frac{\partial^2 T_1'}{\partial y^2}-\bar{V}\frac{\partial T_1'}{\partial y}-iT_1'=-\left(\frac{\gamma-1}{\gamma}\right)\bar{u}\frac{\partial p'}{\partial x}+\bar{u}\frac{\partial T_0'}{\partial x} \quad (17)$$

with

$$u_1'(0)=T_1'(0)=0$$

and

$$u_1'(\infty)=\bar{u}_c\frac{p'}{\gamma}, \quad T_1'(\infty)=0$$

It should be noted that v' in Eq. (16) should also be known to zeroth order. It will be obtained as the solution of an integral equation as described later.

The solutions for u_1' and T_1' may be written in terms of the Green's function G[4,9] satisfying the adjoint problem

$$\frac{\partial^2 G}{\partial y^2}+\bar{V}\frac{\partial G}{\partial y}-iG=-\delta(y-y_0)$$

with

$$G(0)=G(\infty)=0$$

whereby

$$u_1' = -\int_0^\infty G(y_0;y)\,\frac{\partial \bar{u}}{\partial y_0}\,(v'+\bar{V}p'-\bar{V}T_0')\,dy_0 - \int_0^\infty G(y_0;y)\bar{u}\,\frac{\partial u_0'}{\partial x}\,dy_0 \tag{18}$$

and

$$T_1' = \int_0^\infty G(y_0;y)\bar{u}\,\frac{\partial p'}{\partial x}\,dy_0 - \int_0^\infty G(y_0;y)\bar{u}\,\frac{\partial T_0'}{\partial x}\,dy_0 \tag{19}$$

Using standard methods,[9] $G(y_0;y)$ turns out to be

$$G(y_0;y) = \frac{1}{m_2-m_1}[e^{-m_1y_0}e^{m_2y} - e^{-m_2y_0}e^{m_2y}], \quad y_0<y$$

$$= \frac{1}{m_2-m_1}[e^{-m_1y_0}e^{m_2y} - e^{-m_1y_0}e^{m_1y}], \quad y_0>y$$

with

$$m_1 = \frac{\bar{V}+\sqrt{\bar{V}^2+4i}}{2} \quad \text{and} \quad m_2 = \frac{\bar{V}-\sqrt{\bar{V}^2+4i}}{2}$$

Utilizing Eqs. (14) and (15) in Eqs. (18) and (19) and the assumed form for $\bar{u}$ from Eq. (7), one obtains

$$T_1' = \bar{u}_c\left(\frac{\gamma-1}{\gamma}\right)\frac{dp'}{dx}[e^{m_2y}(\alpha_2-\alpha_4)+\alpha_4e^{-(\beta+\beta_2)y}-\alpha_2e^{-\beta y}] \tag{20}$$

where

$$\alpha_2 = 1/(\beta+m_1)(\beta+m_2)$$

and

$$\alpha_4 = 1/(\beta+\beta_2+m_1)(\beta+\beta_2+m_2)$$

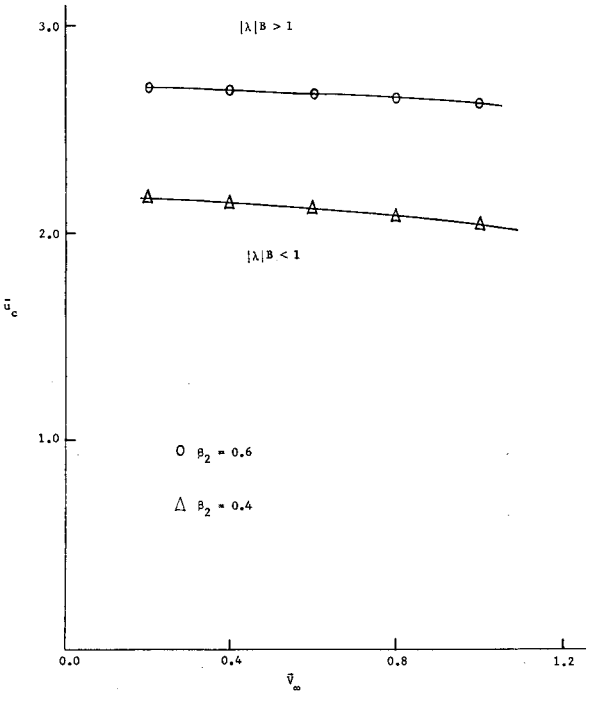

Fig. 2 Region of convergence for the solution of the integral equation for v'.

and

$$u_1' = \frac{i\bar{u}_cp'}{\gamma}\left[\frac{1}{i}+\alpha_1e^{m_2y}+\alpha_2e^{-\beta y}+\alpha_3e^{-\beta_2y}-\alpha_4e^{-(\beta+\beta_2)y}\right] - \int_0^\infty G(y_0;y)\,\frac{\partial \bar{u}}{\partial y_0}[v'+\bar{V}p'-\bar{V}T_0']\,dy_0 \tag{21}$$

where

$$\alpha_3 = 1/(\beta_2+m_1)(\beta_2+m_2)$$

and

$$\alpha_1 = \alpha_4-\alpha_3-\alpha_2-(1/i)$$

To solve for v', Eq. (8) is integrated from 0 to y retaining terms only to $\mathcal{O}(M)$. Substituting for u' and T' and carrying out the integration yields, after some rearrangement,

$$\begin{aligned} v' = {} & v'(x,0)+p'(1-e^{-\beta y})\left[\left(\frac{\gamma-1}{\gamma}\right)\bar{V}-\frac{i}{\beta}\right] \\ & + \bar{V}T_1' - \frac{\bar{u}_c}{\gamma}\frac{dp'}{dx}\left\{\frac{e^{m_2y}}{m_2}[i\alpha_1-i(\gamma-1)(\alpha_2-\alpha_4)]\right. \\ & + \left(\frac{e^{-(\beta+\beta_2)y}}{(\beta+\beta_2)}-\frac{e^{-\beta y}}{\beta}\right)(i\gamma+\gamma-1) - \frac{e^{-\beta_2y}}{\beta_2}(i\alpha_3-1) \\ & + \frac{1}{\beta_2}(i\alpha_3-1)+\left(\frac{1}{\beta}-\frac{1}{\beta+\beta_2}\right)(i\gamma+\gamma-1) \\ & \left. - \frac{1}{m_2}[i\alpha_1-i(\gamma-1)(\alpha_2-\alpha_4)]\right\} \\ & + \frac{\bar{V}}{\gamma}\frac{dp'}{dx}\int_0^y\int_0^\infty G(y_0;\eta)\frac{\partial \bar{u}}{\partial y_0}[1+(\gamma-1)e^{-\beta y_0}]\,dy_0\,d\eta \\ & + \int_0^y\int_0^\infty G(y_0;\eta)\frac{\partial \bar{u}}{\partial y_0}\frac{\partial v'}{\partial x}\,dy_0\,d\eta \\ & - \left[\frac{i}{\gamma}\left(\frac{d^2p'}{dx^2}+p'\right)+\frac{2\bar{u}_c}{\gamma}\frac{dp'}{dx}\right]y \end{aligned} \tag{22}$$

Since v' must remain bounded as $y\to\infty$, a condition on the admissible values of p' is obtained by setting the coefficient of y on the right-hand side of Eq. (22) to zero, that is

$$i\left(\frac{d^2p'}{dx^2}+p'\right)+2\bar{u}_c\frac{dp'}{dx}=0$$

which yields

$$p' \sim e^{\pm ix}e^{i\bar{u}_cx}$$

This solution for p' is consistent with the solution for the acoustic pressure distribution in a duct with slowly varying mean axial flow.

To simplify Eq. (22), the two double integrals on the right-hand side are converted to single integrals by interchanging the order of integration. This process yields

$$\frac{\bar{V}}{\gamma}\frac{dp'}{dx}\int_0^y\int_0^\infty G(y_0;\eta)\frac{\partial \bar{u}}{\partial y_0}[1+(\gamma-1)e^{-\beta y_0}]\,dy_0\,d\eta = \frac{\bar{V}}{\gamma}\frac{dp'}{dx}\int_0^\infty K(y_0;y)\frac{\partial \bar{u}}{\partial y_0}[1+(\gamma-1)e^{-\beta y_0}]\,dy_0$$

and

$$\int_0^y \int_0^\infty G(y_0;\eta)\frac{\partial \bar{u}}{\partial y_0}\frac{\partial v'}{\partial x}\,dy_0 d\eta = \int_0^\infty K(y_0;y)\frac{\partial \bar{u}}{\partial y_0}\frac{\partial v'}{\partial x}\,dy_0$$

where

$$K(y_0;y) = \frac{1}{m_2 - m_1}\left[e^{-m_1 y_0}\left(\frac{1}{m_1} - \frac{1}{m_2} + \frac{e^{m_2 y}}{m_2}\right) - \frac{e^{-m_2 y_0}e^{m_2 y}}{m_2} + \frac{1}{m_2} - \frac{1}{m_1}\right], \quad y_0 < y$$

$$K(y_0;y) = \frac{1}{m_2 - m_1}\left[e^{-m_1 y_0}\left(\frac{1}{m_1} - \frac{1}{m_2} + \frac{e^{m_2 y}}{m_2} - \frac{e^{m_1 y}}{m_1}\right)\right], \quad y_0 > y$$

Substituting the above expression into Eq. (22) yields an integral equation of the form

$$v'(x,y) = F(x,y) + \lambda\int_0^\infty K(y_0;y)\frac{\partial v'}{\partial x}\,dy_0 \tag{23}$$

To establish convergence, it is convenient to multiply both sides of Eq. (23) by $\exp(-\beta_2 y/2)$. With some rearrangement, this equation becomes

$$q(x,y) = F_1(x,y) + \lambda\int_0^\infty L(y_0;y)\frac{\partial q}{\partial x}\,dy_0 \tag{24}$$

where

$$\lambda = \beta_2 \bar{u}_c, \quad q(x,y) = e^{-\beta_2 y/2}v'(x,y)$$

$$F_1(x,y) = e^{-\beta_2 y/2}F(x,y)$$

and

$$L(y_0;y) = e^{-\beta_2 y/2}e^{-\beta_2 y_0/2}K(y_0;y)$$

Using the method of successive approximations,[10] it may be shown by direct substitution that the solution for q is given by

$$q = F_1(x,y) + \sum_{m=1}^{\infty}\lambda^m\int_0^\infty L_m(y_0;y)\frac{\partial^m F_1}{\partial x^m}\,dy_0 \tag{25}$$

where

$$L_m(y_0;y) = \int_0^\infty L(\tilde{y};y)L_{m-1}(y_0;\tilde{y})\,d\tilde{y}$$

and

$$L_1(y_0;y) = L(y_0;y)$$

provided the series in Eq. (25) converges. It may be also shown, using arguments similar to these in Ref. 10, that a sufficient condition for convergence is

$$|\lambda| B < 1$$

where

$$B^2 = \int_0^\infty \int_0^\infty |L(y_0;y)|^2\,dy\,dy_0$$

When $|\lambda|\beta < 1$, the series in Eq. (25) converges faster than the geometric series with the common ratio $|\lambda|\beta$. A typical region of convergence is plotted in Fig. 2. When $|\lambda|\beta \ll 1$, as occurs when the core flow Mach number is small, the convergence is rapid. In such a case, the solution for v' to first order in the Mach number is given by

$$\begin{aligned} v'(x,y) = {} & v'(x,0) + p'(1-e^{-\beta y})\left[\left(\frac{\gamma-1}{\gamma}\right)\bar{V} - \frac{i}{\beta}\right] \\ & + \bar{V}\bar{u}_c\left(\frac{\gamma-1}{\gamma}\right)\frac{dp'}{dx}[e^{m_2 y}(\alpha_2 - \alpha_4) + \alpha_4 e^{-(\beta+\beta_2)y} - \alpha_2 e^{-\beta y}] \\ & + \beta_2\bar{u}_c\frac{dp'}{dx}\left[R_b(0) + \bar{V} - \frac{i}{\beta}\right]\left[\frac{\alpha_3 e^{-\beta_2 y}}{\beta_2} - \frac{1}{m_2\beta_2(m_1+\beta_2)} + \frac{\alpha_3 e^{m_2 y}}{m_2}\right] \\ & + \beta_2\bar{u}_c\frac{dp'}{dx}\frac{i}{\beta}\left[\frac{\alpha_4 e^{-(\beta+\beta_2)y}}{(\beta+\beta_2)} - \frac{1}{m_2(\beta_2+\beta)(\beta_2+\beta+m_1)} + \frac{\alpha_4 e^{m_2 y}}{m_2}\right] \\ & - \frac{\bar{u}_c}{\gamma}\frac{dp'}{dx}\left\{\frac{e^{m_2 y}}{m_2}[i\alpha_1 - i(\gamma-1)(\alpha_2-\alpha_4)]\right. \\ & + \left(\frac{e^{-(\beta+\beta_2)y}}{\beta+\beta_2} - \frac{e^{-\beta y}}{\beta}\right)(i\gamma+\gamma-1) - \frac{e^{-\beta_2 y}}{\beta_2}(i\alpha_3 - 1) \\ & + \frac{1}{\beta_2}(i\alpha_3 - 1) + \left(\frac{1}{\beta} - \frac{1}{\beta+\beta_2}\right)(i\gamma+\gamma-1) \\ & \left. - \frac{1}{m_2}[i\alpha_1 - i(\gamma-1)(\alpha_2-\alpha_4)]\right\} \end{aligned} \tag{26}$$

where it is assumed that the wall admittance $R_b(0)$ is independent of x.

Utilizing Eq. (26) in Eq. (21) and using Eq. (14), the solution for u' becomes

$$\begin{aligned} u'(x,y) = {} & \frac{i}{\gamma}\frac{dp'}{dx}(1-e^{-\beta y}) \\ & + \frac{i\bar{u}_c p'}{\gamma}\left[\frac{1}{i} + \alpha_1 e^{m_2 y} + \alpha_2 e^{-\beta y} + \alpha_3 e^{-\beta_2 y} - \alpha_4 e^{-(\beta+\beta_2)y}\right] \\ & - \beta_2\bar{u}_c p'\left[R_b(0) + \bar{V} - \frac{i}{\beta}\right][e^{m_2 y} - e^{-\beta_2 y}]\alpha_3 \\ & - \frac{i\beta_2\bar{u}_c p'}{\beta}[e^{m_2 y} - e^{-(\beta+\beta_2)y}]\alpha_4 \end{aligned} \tag{27}$$

It is to be noted that if the effects of the mean flow velocity $\bar{u}$ are neglected, as done by Flandro,[1] the solutions for u' and v' reduce to the following simpler forms:

$$v'(x,y) = v'(x,0) + p'(1-e^{-\beta y})\left[\left(\frac{\gamma-1}{\gamma}\right)\bar{V} - \frac{i}{\beta}\right] \tag{28}$$

and

$$u'(x,y) = \frac{i}{\gamma}\frac{dp'}{dx}(1-e^{-\beta y}) \tag{29}$$

In this case $v'(x,y)$ has a local minimum when p' is a minimum [since $v'(x,0) = R_b(0)p'$] and $u'(x,y)$ has a minimum when dp'/dx is minimum. However, when the effects of $\bar{u}$ are included, this is no longer true, as will be discussed later.

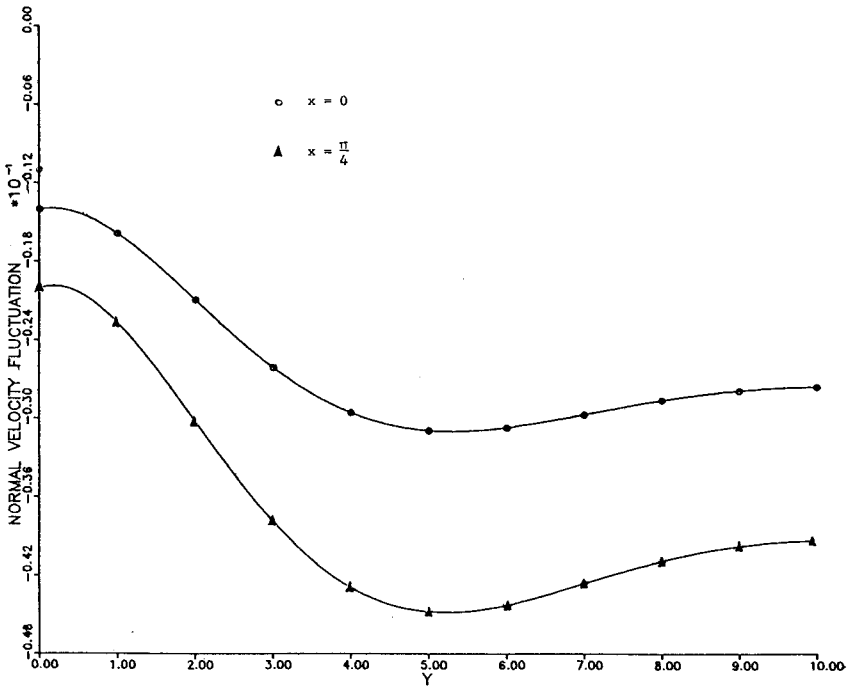

Fig. 3 Variation of Real(v') with normal distance y from the wall at $x=0$ and $\pi/4$.

The side wall admittance that needs to be satisfied by the core flow is obtained by letting $y\to\infty$ in Eq. (26) and dividing by p'. The result is

$$R_b(\infty)=R_b(0)+\left[\left(\frac{\gamma-1}{\gamma}\right)\bar{V}-\frac{i}{\beta}\right]$$
$$-\frac{\beta_2\bar{u}_c}{p'}\frac{dp'}{dx}\left\{\frac{[R_b(0)+\bar{V}-i/\beta]}{m_2\beta_2(m_1+\beta_2)}\right.$$
$$\left.+\frac{i}{\beta m_2(\beta_2+\beta)(\beta_2+\beta+m_1)}\right\}$$
$$-\frac{\bar{u}_c}{\gamma p'}\frac{dp'}{dx}\left\{\frac{1}{\beta_2}(i\alpha_3-1)+\left(\frac{1}{\beta}-\frac{1}{\beta+\beta_2}\right)(i\gamma+\gamma-1)\right.$$
$$\left.-\frac{1}{m_2}[i\alpha_1-i(\gamma-1)(\alpha_2-\alpha_4)]\right\} \tag{30}$$

The thickness of the acoustic boundary layer may be identified with the thickness of the u' boundary layer. The boundary-layer thickness for u' according to Eq. (18) depends on $G(y_0,y)$. When $y\to\infty$, the relevant exponential term in $G(y_0,y)$ is $e^{m_2 y}$. Recalling that

$$m_2=(\bar{V}-\sqrt{\bar{V}^2+4i})/2$$

the boundary layer (bl) thickness for u' may be estimated by setting

$$y_{\rm bl}=\left|\frac{1}{\text{Real}(m_2)}\right|=\frac{1}{a}$$

where

$$a=\frac{\bar{V}}{2\sqrt{2}}\left(1+\sqrt{1+\frac{16}{\bar{V}^4}}\right)^{1/2}-\frac{\bar{V}}{2} \tag{31}$$

For the boundary-layer equations to be valid, the thickness of the acoustic boundary layer should be much smaller than the characteristic transverse dimension of the duct. Hence, before application of the theory, this condition should be verified. It should be noted that the boundary-layer thickness increases with increase in the injection velocity. For the case of $V^*=0$, it is straightforward to show that Eq. (31) reduces to

$$y^*_{\rm bl}=\sqrt{2\nu^*/\omega^*}$$

in accordance with classical results.[4]

Discussion of Results

The variation of v' and u' in the boundary layer may be directly obtained from Eqs. (26) and (27). The important quantity, insofar as the transfer of acoustic energy between the core flow acoustic motion and the boundary-layer oscillations, is the part of v' in phase with the pressure p' at the edge of the boundary layer. If p' and $v'(\infty)$ are in phase, acoustic energy is transferred to the core flow acoustic motion. Calculations show that v' in the boundary layer depends on $v'(0)$ [and so also on $R_b(0)$], p', and $\bar{V}$. A porous wall usually acts as a damper for acoustic motions, which would imply with the present notation that the real part of $R_b(0)$ is negative. Sample calculations are therefore carried out for negative values of $R_b(0)$.

Figure 3 describes the y variation of the real part of v' at two different axial locations. In this calculation, p' is taken to vary as $0.01[e^{i(\bar{u}_c+x)}+e^{i(\bar{u}_c-x)}]$ with $\bar{u}_c=0.05$, so that p' is almost purely real. The two axial locations are taken at $x=0$ and $\pi/4$. The values of the other parameters were taken to be $\bar{V}=1.0$, $\beta_2=0.6$, and $R_b(0)=-1.0$. At these two x locations, away from a pressure minimum, the effect of the $\bar{u}$ terms is negligible and there is no significant difference between Eqs. (26) and (28). At these locations, the effect of the boundary layer is to further enhance the damping provided by the porous wall. In Fig. 4, the variation of v' across the boundary layer at a location of pressure minimum (i.e., $x=\pi/2$) is presented. At this location if p' is identically zero then according to Flandro's calculation [Eq. (28)], v' remains identicallly zero. However, by inclusion of the $\bar{u}$ terms, it is seen that v' is different from zero at a pressure minimum.

As mentioned before, the important energy exchange between the core and boundary-layer flows depends upon the

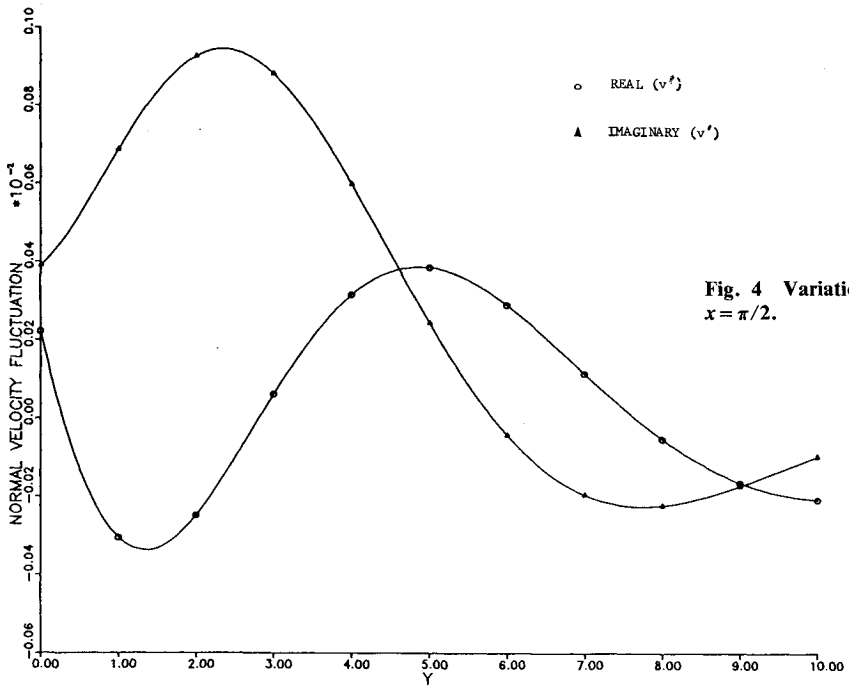

Fig. 4 Variation of v' with normal distance y from the wall at $x=\pi/2$.

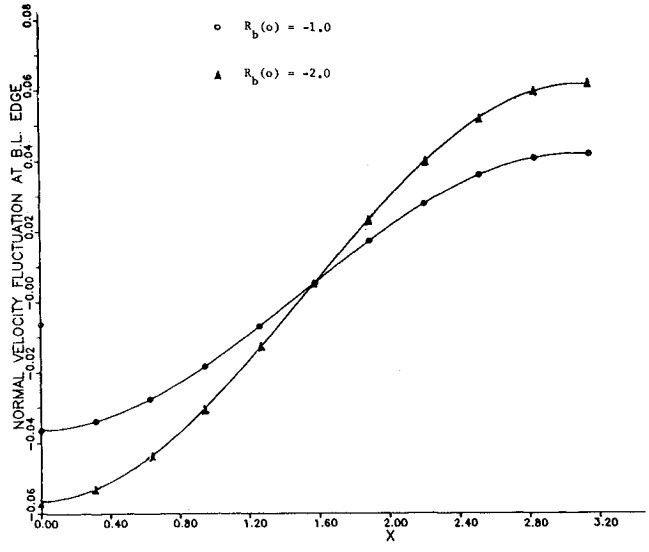

Fig. 5 Dependence of Real$v'(\infty)$ upon location within duct for $R_b(0)=-1.0$ and -2.0.

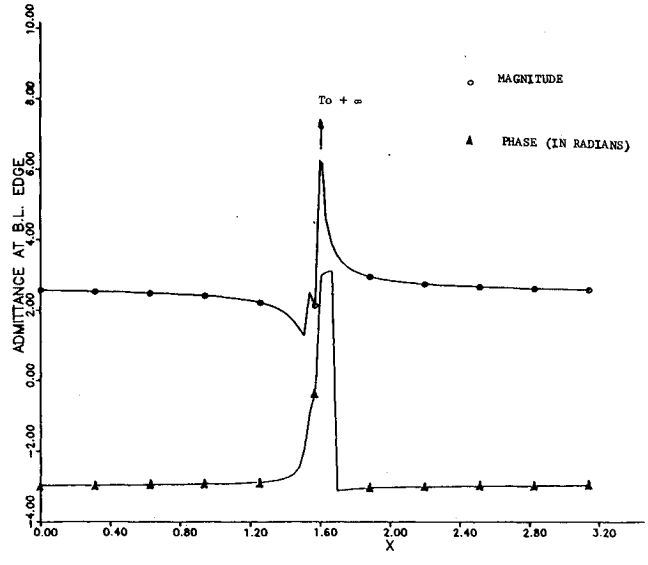

Fig. 6 Dependence of $R_b(\infty)$ upon x location within duct.

part of v' in phase with p'. Since here p' is almost purely real, it is the real part of v' at the boundary-layer edge that is important. The dependence of Real $[v'(\infty)]$ upon $R_b(0)$ is presented in Fig. 5 as a function of axial distance x. Two values of $R_b(0)$ are chosen (-1.0 and -2.0). The other parameters retain the values given previously. The magnitude of Real$v'(\infty)$ increases with $R_b(0)$ is changed from -1.0 to -2.0. For $0<x<\pi/2$, Real$v'(\infty)$ becomes more negative and for $\pi/2<x<\pi$, Real$v'(\infty)$ becomes more positive as $R_b(0)$ changes from -1.0 to -2.0. As p' is positive for $0<x<\pi/2$ and negative for $\pi/2<x<\pi$, it follows that, when the wall is more damping [i.e., $R_b(0)$ is more negative], the damping at the edge of the boundary layer is also higher. It should be pointed out, however, that the increase in damping at the boundary-layer edge is not linearly proportional to the increase in $R_b(0)$.

However, $v'(\infty)$ does not go to zero exactly at the pressure minimum and, in fact, in a small region near the minimum v' and p' can be in phase, indicating energy transfer from the boundary-layer oscillations to the core flow acoustic motions. This can be seen more clearly by looking at the admittance $R_b(\infty)$ at the edge of the boundary layer for $0<x<\pi$ (Fig. 6). The magnitude and phase are relatively constant away from the pressure minimum ($x=\pi/2$). However, there is a strong axial dependence in the vicinity of the pressure minimum. The phase between v' and p' approaches zero in a small neighborhood of the pressure minimum and the magnitude approaches infinity, if p' is identically zero at the minimum. However, the acoustic energy transfer to the core flow oscillations [here given by $\overline{p'\text{Real}v'(\infty)}$] in the vicinity of the pressure minimum remains small.

The dependence of Real$v'(\infty)$ upon $\bar{V}$ is similar to its dependence upon $R_b(0)$ (Fig. 7). Increase in $\bar{V}$ implies an increase in the steady flow injection rate and the acoustic boundary-layer thickness. Therefore, increasing the injection

flow rate increases the damping of the core flow oscillations by the acoustic boundary layer.

In an effort to check the trends predicted by the theory, experimental studies were carried out in a cylindrical porous walled duct. The duct was constructed by joining cylindrical porous sleeves, each measuring 30 cm in length and 5 cm in diameter. The head end ($x=0$) was capped, while the tail end exhausted through a nozzle into a vacuum tank. The flow rate was adjusted by means of a valve located between the nozzle and the vacuum tank. An acoustic driver (capable of driving at different frequencies) was located at the head end. Profiles of u' were obtained in the acoustic boundary layer by means of a hot-film anemometer. The measured ratio $|u'(y)/u'(\infty)|^2$ is plotted in Fig. 8 for flow rates of approximately 0.3 and 0.5 m/s ($V=3.11$ and 5.19, respectively) at a frequency of 100 Hz. Due to the axial pressure drop along the duct, the injection was not uniform and the average injection rate was determined by measuring the flow rate at the nozzle end. The value of $u'(\infty)$ was taken at the duct centerline. Also plotted for comparison are the corresponding theoretical profiles. These were obtained by using Eq. (29) as the axial location under consideration was at $x=25$ cm, which was sufficiently removed from a pressure minimum.

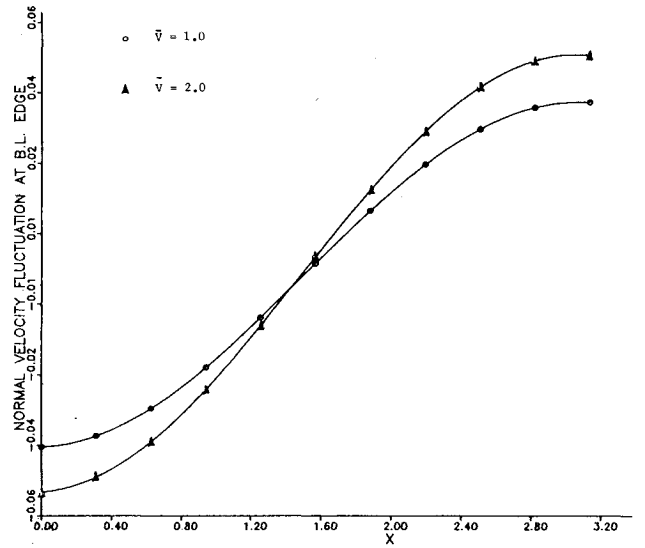

Fig. 7 Dependence of Real$v'(\infty)$ upon x location within duct for $V=1.0$ and 2.0.

Figure 8 shows that the developed model predictions are in good qualitative agreement with the experimental data. In particular, the increase in the boundary-layer thickness with increase in injection flow rate is clearly evident. The quantitative agreement between theory and experiment is also reasonable. The theoretical values of $|u'(y)/u'(\infty)|^2$ are about a factor of 1.4 greater than the experimentally obtained data, so that the magnitude of $u'(y)$ differs only by a factor of 1.2.

It is also interesting to note from Fig. 8 that there is a region in the boundary layer where the unsteady fluid velocity u' is larger than in the core flow $u'(\infty)$. This phenomenon is known to be present in ducts with no mean flow and is called the Richardson's annular effect.[11] The present investigation confirms both theoretically and experimentally that this effect is also present in ducts with mean flow and sidewall flow injection. As explained in Refs. 4 and 11, this effect occurs due to the presence of the vortical mode of the fluid motion, which must arise in the boundary layer to satisfy the no-slip boundary condition at the duct walls that the isentropic acoustic mode by itself cannot satisfy.

It has been stated earlier that the analysis has been carried out for largely plane wave motions in the duct interior [i.e., see Eq. (5)]. It has also been shown that v' at the edge of the acoustic boundary layer is, in general, nonzero. However, at the duct centerline v' must go to zero. A similar situation occurs in the case of nonporous and nonrigid walled ducts with no steady flow. It is shown[4] that in this case the acoustic motions are not perfect plane waves and the acoustic pressure shows a weak radial dependence, enough to sustain a radial acoustic velocity in the duct interior that goes to zero at the duct centerline. The situation in the present case should be no different and it must be recognized that Eq. (5) is the first approximation to the actual case.

Summary

A theoretical analysis and an experimental study of the acoustic boundary layer in porous-walled ducts with sidewall mass injection have been carried out. The analysis shows the damping provided by the acoustic boundary layer increases with an increase in injection velocity and increased damping at the wall. For a given injection velocity, the thickness of the boundary layer decreases with an increase in the frequency of the oscillations. The thickness of the boundary layer increases with increase in injection velocity. This important trend is also confirmed experimentally. The ex-

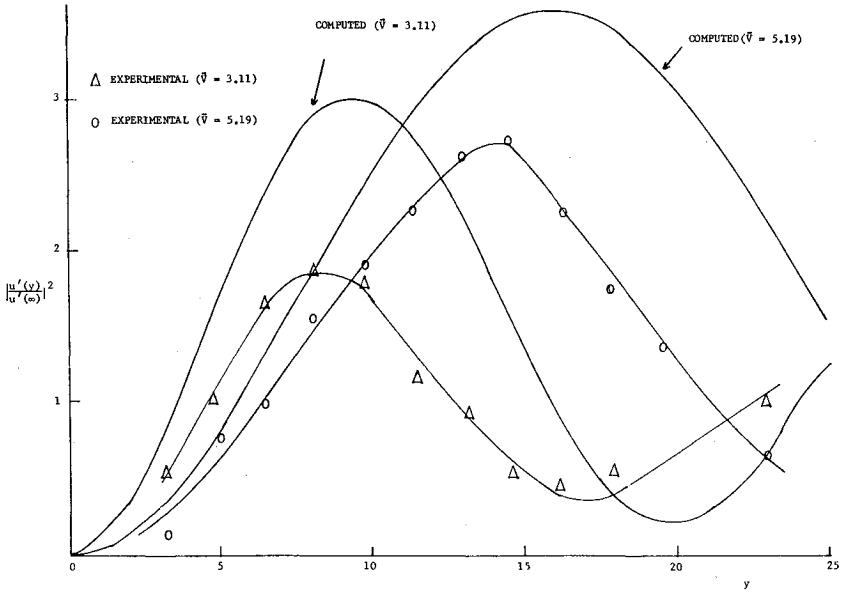

Fig. 8 Comparison of measured and predicted dependence of $|u'(y)/u'(\infty)|^2$ on normal distance y from the wall.

perimental data are in good agreement with the theoretical predictions.

References

[1]Flandro, G. A., "Solid Propellant Acoustic Admittance Corrections," *Journal of Sound and Vibration*, Vol. 36, 1974, pp. 297-312.

[2]Hegde, U. G. and Strahle, W. C., "Sound Generation by Turbulence in Simulated Rocket Motor Cavities," *AIAA Journal*, Vol. 23, Jan. 1985, pp. 71-77.

[3]Pierce, A. D., *Acoustics*, McGraw-Hill Book Co., New York 1982.

[4]Morse, P. M. and Ingard, K. U., *Theoretical Acoustics*, McGraw-Hill Book Co., New York, 1968.

[5]T'ien, J. S., "Oscillatory Burning of Solid Propellants Including Gas Phase Time Lag," *Combustion Science and Technology*, Vol. 5, 1972, pp. 47-54.

[6]Flandro, G. A., "Nonlinear Time Dependent Combustion of a Solid Rocket Propellant," College of Engineering, University of Utah, Salt Lake City, Rept. UTEC ME 82-087, 1982.

[7]Nayfeh, A. H., "Effect of the Acoustic Boundary Layer on the Wave Propagation in Ducts," *Journal of the Acoustical Society of America*, Vol. 59, 1973, pp. 1737-1742.

[8]Schlichting, H., *Boundary-Layer Theory*, 7th ed., McGraw-Hill Book Co., New York, 1979.

[9]Churchill, R. V., *Operational Mathematics*, 3rd ed., McGraw-Hill Book Co., New York, 1972.

[10]Kanwal, R. P., *Linear Integral Equations*, Academic Press, New York, 1972.

[11]Temkin, S., *Elements of Acoustics*, John Wiley & Sons, New York, 1981.